High-Activity, Durable Oxygen Reduction Electrocatalyst: Nanoscale Composite of Platinum–Tantalum Oxyphosphate on Vulcan Carbon

5 AUTHORS, INCLUDING:

Yannick Garsany
United States Naval Research Laboratory
35 PUBLICATIONS **551** CITATIONS

Albert Epshteyn
United States Naval Research Laboratory
26 PUBLICATIONS **213** CITATIONS

Andrew P Purdy
United States Naval Research Laboratory
34 PUBLICATIONS **586** CITATIONS

Karen E. Swider-Lyons
United States Naval Research Laboratory
**105** PUBLICATIONS **1,531** CITATIONS

High-Activity, Durable Oxygen Reduction Electrocatalyst: Nanoscale Composite of Platinum–Tantalum Oxyphosphate on Vulcan Carbon

Yannick Garsany,*,[†,‡] Albert Epshteyn,[†] Andrew P. Purdy,[†] Karren L. More,[§] and Karen E. Swider-Lyons[†]

[†]Naval Research Laboratory, Chemistry Division, 4555 Overlook Avenue Southwest, Washington, D.C. 20375, [‡]EXCET INC., 8001 Braddock Road, Suite 105, Springfield, Virginia 22151, and [§]Oak Ridge National Laboratory, Oak Ridge, Tennessee 37831

ABSTRACT A new oxygen reduction electrocatalyst for proton-exchange membrane fuel cells (PEMFCs) is synthesized by dispersing nanoscale Pt on a nanoscale tantalum oxyphosphate phase on a Vulcan carbon support, designated as $Pt/[TaOPO_4/VC]$. Electrocatalytic activity is measured by the thin-film rotating disk electrode methodology in 0.1 M $HClO_4$ electrolyte. The $Pt/[TaOPO_4/VC]$ electrocatalyst has a high mass-specific activity of 0.46 A mg^{-1}_{Pt} compared to 0.20 A mg^{-1}_{Pt} for a Pt/Vulcan carbon standard and has met the 2015 DOE goal of 0.44 A mg^{-1}_{Pt}. This tantalum-containing electrocatalyst is twice as durable as the standard Pt/carbon in terms of its loss of Pt electrochemical surface area after aggressive electrochemical cycling.

SECTION Surfaces, Interfaces, Catalysis
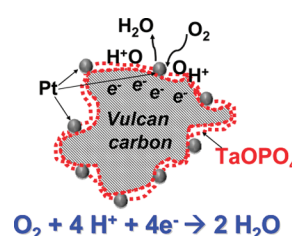
Platinum-based electrocatalysts are the most active for the oxygen reduction reaction (ORR) at the cathode of low-temperature fuel cells, that is, proton-exchange membrane fuel cells (PEMFCs). These oxygen reduction electrocatalysts typically comprise nanoparticles of platinum and platinum alloys supported on high-surface-area carbon substrates (e.g., Vulcan carbon XC72, VC, or other graphitized carbons).[1] The kinetics of these electrocatalysts are still inadequate, and they suffer from a 400 mV overpotential from the equilibrium reversible potential (1.20 V at 80 °C) under typical PEMFC operating conditions. The stability of these Pt-based ORR electrocatalysts is a major concern due to corrosion of the Pt and carbon at the high potentials of the cathode.[2,3]

Platinum nanoparticles supported on metal oxides MO_x (M = Ti, Ce, Mo, W, Nb, Ta) have enhanced electrocatalytic activities toward the ORR.[4−13] The oxide can affect the electrocatalytic activity of the supported noble metal due to metal–support interactions through modification of the electronic states or the Fermi level of the Pt[14], by preferential adsorption of the OH groups to the oxide versus the Pt surface[9] or reduced OH adsorption caused by lateral repulsion between Pt−OH and oxide surface species.[8] Recent experiments performed by our group showed that the specific catalytic activity of a platinum-based electrocatalyst was enhanced when dispersed on tantalum oxide.[9] We have also studied extensively the enhancement of Pt activity when dissolved in or supported on metal phosphates (FePO or $FePO_4$).[15,16] Hydrous phosphates were chosen because they are more stable to dissolution than oxides and can also be good proton conductors.[17] However, iron phosphates are somewhat soluble in hot acids, indicating that they are a poor choice for a practical PEMFC. In order to address chemical stability issues, our efforts have turned to platinum–tantalum oxyphosphate. Tantalum is used as a screen and catalyst support in the anodes of acidic electrolyzers and is significantly more stable than any transition metal or rare earth oxides under the harsh conditions of electrolyzers.

We present here a high-activity and durable ORR electrocatalyst created by impregnating the platinum nanoparticles on a nanoscale tantalum oxyphosphate coating on the Vulcan carbon support, designated as $Pt/[TaOPO_4/VC]$. The catalyst is designed with a Pt nanoparticle loading of 18 % and a thin film of tantalum oxyphosphate in contact with the Vulcan carbon support, where the tantalum accounts for 3 wt % and the phosphorus for 1 wt % of the catalyst weight. The ORR activity results are compared to a standard 20 % Pt/Vulcan carbon catalyst, which most closely matches our catalyst composition and carbon support. Thin-film RDE methodology[18,19] is used to determine the electrocatalyst Pt electrochemical surface area (ECSA) and ORR activity in terms of mass-specific and area-specific ORR activities. Durability measurements are carried out on the same 20 % Pt/VC standard, as well as a commercial 47.3 % Pt standard on graphitized carbon.

Figure 1 displays a high-angle annular dark field scanning transmission electron microscopy (HAADF-STEM) image of a $Pt/[TaOPO_4/VC]$ catalyst heated to 660 °C. Ta is resolved as single atoms. The Ta is a part of a subnanometer, amorphous film. The Ta phase appears to be an amorphous oxide film with no distinctive $TaOPO_4$ phase. It is dispersed across
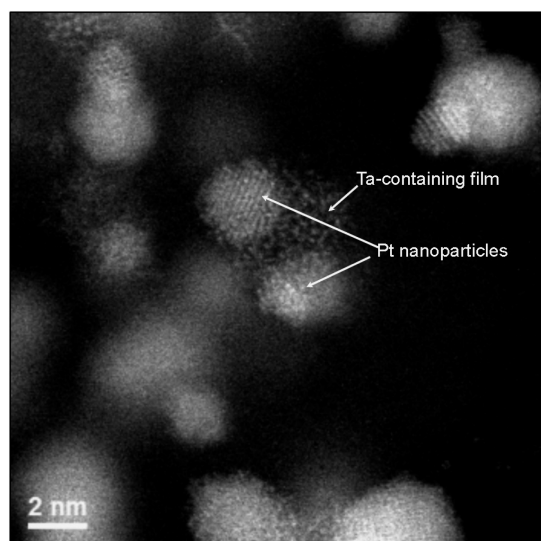
Figure 1. HAAD-STEM image of Pt nanoparticles on TaOPO$_4$ on Vulcan carbon.

the carbon surface between the Pt particles as amorphous clusters. The Pt particles are only 2.4 nm in diameter, even after heating to 660 °C, as compared to 6 nm for Pt/Vulcan carbon catalysts heated to the same temperature.

Use of the RDE thin-film method for the electrochemical characterization of the Pt/[TaOPO$_4$/VC] eletrocatalyst is first validated by the Levich and Koutecký−Levich analysis. These results are shown and discussed in the Supporting Information and confirm that thin films of our electrocatalysts perform well for the ORR, with a negligible contribution from O$_2$ diffusion through the Nafion film and the Pt/[TaOPO$_4$/VC] film layer. The reaction is shown to be a four-electron process, confirming efficient oxygen reduction.

Figure 2a compares the ORR polarization curves measured for a thin film of our 18 wt % Pt/[TaOPO$_4$/VC] electrocatalyst compared to that of a 20 wt % Pt/Vulcan carbon. The activity of the Pt/[TaOPO$_4$/VC] electrocatalyst is significant, as indicated by the high onset potential of O$_2$ reduction (0.97−1.03 V) as well as the high half-wave potential ($E_{1/2}$), that is, 0.92 V versus RHE measured at the 1600 rpm rotation rate. The E versus log $|J_k|$ curves or Tafel plots for the ORR normalized to the Pt loading (i.e., mass-specific activity) are shown in inset b of Figure 2 for the two electrocatalysts. The Tafel polarization curves shown in Figure 2b can be fitted to two Tafel regions at low current density (lcd, E > 0.86 V) and high current density (hcd, E < 0.86 V) using the previously established methods.[20,21] The Tafel slopes for both catalysts are well-defined at ∼70 mV dec^{-1} for the low current density region and ∼110 mV dec^{-1} for the high current density region, which suggests that the presence of tantalum oxyphosphate does not change the oxygen activation, which is the limiting step in the ORR mechanism on platinum. They are also in good agreement with Tafel slopes reported in the literature for 46 % Pt/HSC-E (TKK),[1] polycrystalline platinum,[21] and carbon-supported Pt catalysts.[20] The Tafel plots also show that the trend in the catalytic activity for the ORR is Pt/[TaOPO$_4$/VC] ≫ Pt/Vulcan carbon.
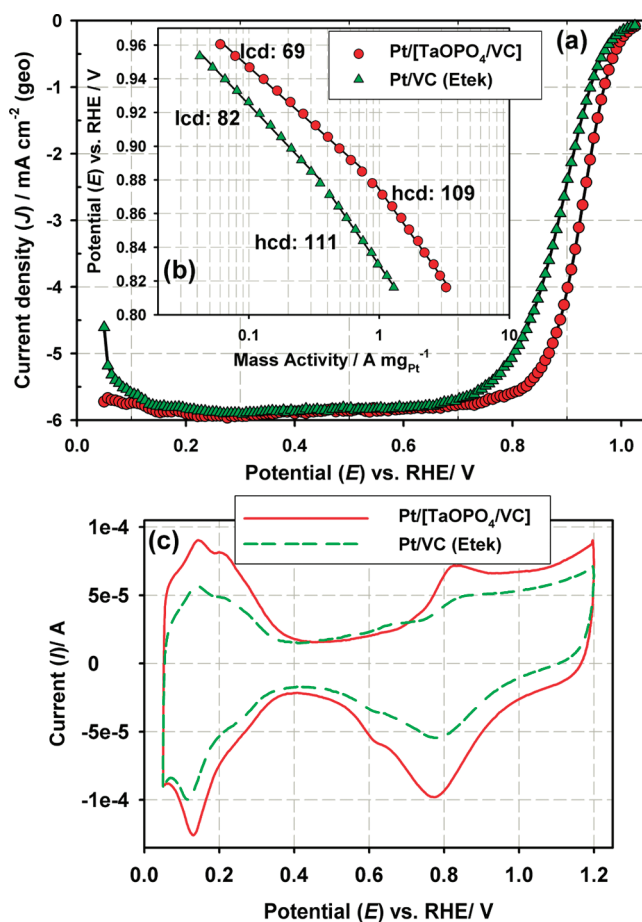

Figure 2. (a) Comparison of ORR polarization curves recorded for 20 % Pt/VC (green triangle) and Pt/[TaOPO$_4$/VC] electrocatalysts (red circle) in O$_2$-saturated 0.1 M HClO$_4$ electrolyte at 30 °C, 1600 rpm, and 20 mV s^{-1}. Anodic scans shown. (b) E versus log $|J_k|$ curves or Tafel plots. Kinetic currents were extracted from the anodic polarization curves presented in (a) and normalized to the Pt loading. (c) CVs of 20 % Pt/Vulcan carbon (Etek) and 18 % Pt/[TaOPO$_4$/VC] in N$_2$-saturated 0.1 M HClO$_4$ at 30 °C recorded at 20 mV s^{-1}.

Cyclic voltammetry (CV) results were used to calculate the electrochemically active Pt surface area (ECSA) of the Pt electrocatalysts. CVs for the Pt/[TaOPO$_4$/VC] (red solid line) and the 20 % Pt/Vulcan carbon (green dash line) electrocatalysts are shown in Figure 2c. Note that on the anodic sweep, the onset for OH adsorption on the Pt region near 0.80 V versus RHE, is the same for the Pt/[TaOPO$_4$/VC] and Pt/Vulcan carbon electrocatalysts. The Pt ECSAs are measured by integrating the columbic charge $Q_{H\text{-adsorption}}$ in (C) under the hydrogen adsorption region in the negative-going potential scan (from 0.40 to 0.05 V) on CVs recorded at 20 mV s^{-1} after correction for double-layer charging (by subtracting the current observed at 0.40 V versus RHE from the total current). This method has been validated versus CO adsorption and Cu UPD methods for measuring the Pt ECSA in our laboratory.[22] Table 1 shows that the Pt ECSA of the Pt/[TaOPO$_4$/VC] electrocatalyst is comparable to that of the 20 % Pt/Vulcan carbon electrocatalyst (Etek).

From the ORR and the Pt ECSA results, the mass-specific and area-specific activities are calculated versus the estimated

Table 1. Electrochemical Parameters of Pt/Tantalum Oxyphosphate Electrocatalyst and Pt/Carbon Standards as Measured from Thin-Film Electrodes

catalysts	Pt loading μg_{Pt} cm^{-2}	ECSA m^2 g$^{-1}_{Pt}$	Tafel slopes mV dec^{-1} (lcd/hcd)^a	I_m A mg$^{-1}_{Pt}$ ± std	I_s μA cm$^{-2}_{Pt}$ ± std
Pt/[TaOPO$_4$/VC]	28	76 ± 3	69/109	0.46 ± 0.02	625 ± 46
Pt/VC (ETEK)	20	62 ± 2	82/111	0.20 ± 0.01	335 ± 40
Pt/HSC-E (TKK) ref (1)^b	13	80 ± 2		0.21 ± 0.01	265 ± 25

^{a} lcd/hcd: low current density/high current density. ^{b} ECSA measured at 25 °C and 20 mV s^{-1} in 0.1 M HClO$_4$; mass-specific and area-specific activities measured at 0.90 V versus RHE, 1600 rpm, and 20 mV s^{-1} in O$_2$-saturated 0.1 M HClO$_4$ at 60 °C.
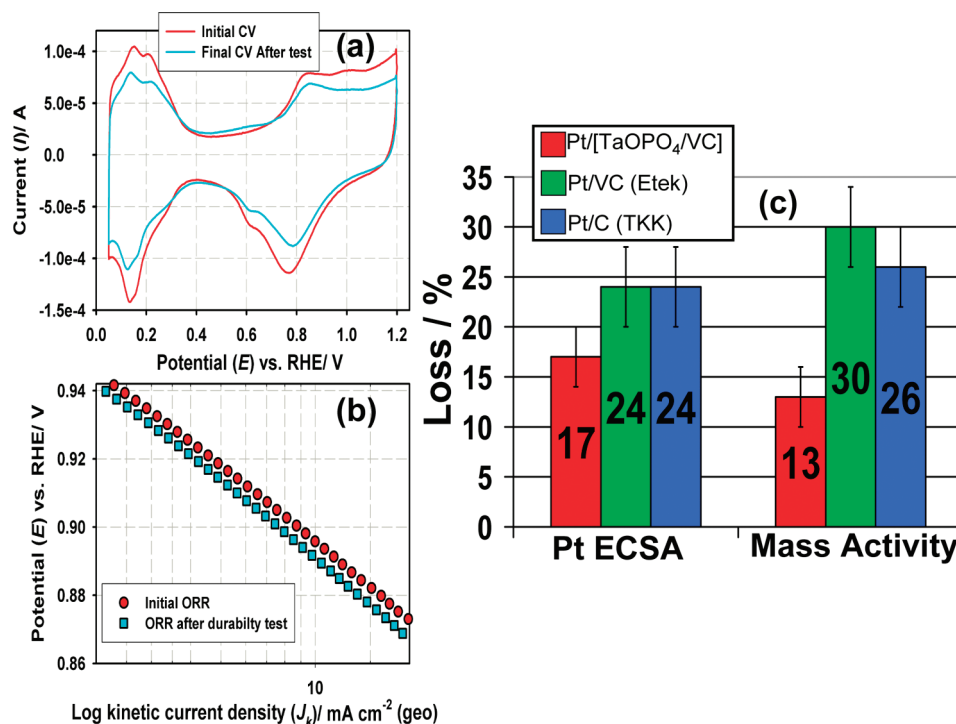

Figure 3. (a) Comparison of CVs recorded before and after durability measurements for the Pt/[TaOPO$_4$/VC] electrocatalyst in N$_2$-saturated 0.1 M HClO$_4$ at 30 °C and a scan rate of 20 mV s^{-1}. (b) Comparison of Tafel plots recorded before and after durability measurements for the Pt/[TaOPO$_4$/VC] electrocatalyst in O$_2$-saturated 0.1 M HClO$_4$ electrolyte at 30 °C, 20 mV s^{-1}, and 1600 rpm. (c) Percentage loss of Pt ECSA and mass-specific activity for Pt/[TaOPO$_4$/VC], Pt/Vulcan carbon (Etek), and Pt/carbon (TKK) electrocatalysts when subjected to oxidation cycles.

Pt loading on the thin-film RDEs. The average of six replicates from six separate thin films and the standard deviation associated with these measurements are presented in Table 1. The mass- and area-specific activities estimated for the commercial electrocatalyst in this study agree well with literature values reported by Gasteiger et al.[1] for state of the art Pt/carbon electrocatalysts. The mass-specific activity at E = 0.90 V versus RHE of the Pt/[TaOPO$_4$/VC] electrocatalyst is 0.46 ± 0.02 A mg$^{-1}_{Pt}$, or ~2.3 × higher than that of the commercial 20% Pt/Vulcan carbon electrocatalyst (0.20 ± 0.02 A mg$^{-1}_{Pt}$). It is also greater than the US DOE 2015 target of 0.44 A mg$^{-1}_{Pt}$. The higher mass-specific activity of the Pt/[TaOPO$_4$/VC] electrocatalyst is apparently due to its high area-specific activity of 625 ± 46 μA cm$^{-2}_{Pt}$, which is ~1.8 times higher than that of the standard (335 ± 40 μA cm$^{-2}_{Pt}$). We have previously demonstrated that TaOPO$_4$/VC (with no platinum) is inactive toward the ORR.[23]

Pt electrochemical surface areas (ECSA) are measured from the Pt−hydrogen desorption region of CVs at 20 mV s^{-1} in

deaerated 0.1 M HClO$_4$ at 30 °C. The Tafel slopes and mass-specific (I_m) and area-specific (I_s) activities are derived from the ORR polarization curves at E = 0.90 V versus RHE, 1600 rpm, and 20 mV s^{-1} in O$_2$-saturated 0.10 M HClO$_4$ at 30 °C.

Figure 3a shows the CVs of the Pt/[TaOPO$_4$/VC] electrocatalyst before and after the 1000 oxidation step cycles between +0.60 (30 s hold) and +1.20 V (30 s hold). For clarity of the figure, only the durability measurement results obtained for the Pt/[TaOPO$_4$/VC] electrocatalyst are presented.

With repeated oxidation cycles, the electrocatalysts exhibited a reduction in various surface-area-dependent processes, the hydrogen adsorption/deposition region (0.05−0.40 V) and the Pt−OH formation/reduction region. This reduction is suggestive of the oxidation of the carbon support at high positive potentials (> 1.0 V) but also could be due to oxidation at the Pt−support interface or to the dissolution of Pt and the growth of Pt particles. However, the Pt/[TaOPO$_4$/VC] electrocatalyst showed better electrochemical stability as determined by lower loss of Pt ECSA, as presented in Figure 3c.

The Pt ECSA was determined from the area under the hydrogen adsorption region in the negative-going potential scan (from 0.40 to 0.05 V) on CVs shown in Figure 3a after correction for double-layer charging (by subtracting the current observed at 0.40 V versus RHE from the total current). Three separate tests were completed for each sample to observe repeatability. The error bar (standard deviation of the three tests) is given for the histogram data, and the average value of ECSA loss is presented in Figure 3c. The Pt/[TaOPO$_4$/VC] electrocatalyst is more stable than the commercial Pt/carbon electrocatalysts, losing 17 % of its initial Pt ECSA compared to the 24 % Pt ECSA loss for the commercial catalysts. Losses in the Pt ECSA are normally on the order of 20 to 70 % during similar potential cycling experiments for catalysts supported on Vulcan carbon.[24] The smaller decrease of the Pt ECSA for the Pt/[TaOPO$_4$/VC] electrocatalyst can be attributed to a better stability of the Pt/Vulcan carbon interface at high positive potentials, with interphase degradation likely structurally mitigated by the tantalum oxyphosphate film.

Measurements of the ORR activity were performed initially and at the end of the durability tests. Figure 3b compares the initial ORR activities to the final ORR activities in the potential region between 0.86 and 0.96 V versus RHE for the Pt/[TaOPO$_4$/VC] electrocatalyst. The observed ORR catalytic activity of the Pt/[TaOPO$_4$/VC] electrocatalyst is barely affected by the durability test. Figure 3c also depicts the loss in mass-specific activities for all three electrocatalysts. The percentage loss in mass activity for the Pt/[TaOPO$_4$/VC] is the smallest at 13 %, whereas it is close to 30 % for both commercial catalysts.

The attributes of Pt nanoparticles are clearly changed when they are supported on Vulcan carbon coated with the tantalum oxyphosphate film, which appears to anchor the Pt nanoparticles. The Pt/[TaOPO$_4$/VC] has higher mass-specific and area-specific activities than Pt/VC standards; however, there does not appear to be an electronic effect, as would be manifested by a shift of the onset potential for Pt–OH adsorption. The Ta phase appears to offer increased durability, possibly because the Ta nanoscale phases are between the Pt and carbon phases or because less Pt oxide is formed on the Pt/[TaOPO$_4$/VC] compared to that on Pt/C. A detailed spectroscopic analysis is underway using in situ X-ray absorption spectroscopy (XAS). We have shown with XAS and electrochemistry that for gold nanoparticles supported on tin oxide, the tin oxide adsorbs oxygen to enable the ORR on gold under acidic conditions.[25,26] Preliminary results for Pt/[TaOPO$_4$/VC] indicate that the tantalum oxyphosphate phase prevents hydroxyl adsorption on the Pt, making more sites available for oxygen reduction. The electrocatalyst might further be improved by optimization of the Pt particle size, tantalum loading, heating conditions, and carbon type.

EXPERIMENTAL METHODS

The nanoscale tantalum oxyphosphate film on the Vulcan carbon was created starting with 80 % H$_3$PO$_4$ (4.4 g) that was dried at 150 °C in a vacuum oven overnight. While in an inert, dry N$_2$ atmosphere, the VC (20 g) was suspended in ethanol (EtOH) (700 mL, 200 proof, USDA grade). The dried polyphosphoric acid was dissolved in EtOH (20 mL), and the solution was added to the VC suspension and sonicated for 2 h while closed with an airtight septum. Ta(EtO)$_5$ in EtOH (10 mL) was then added to the reaction, and it was sonicated overnight. Pt colloids were prepared according to a previously reported method,[27] which was easily scaled to 2 L quantities, much larger than those described in the original reference. Then, 1482 g of Pt colloid (4.4 g Pt) was precipitated with 0.1 M HClO$_4$, resuspended in EtOH (100 mL), and injected into the same flask. The reaction was then sonicated for 2 days. The material was spun at 9300g in a centrifuge and dried under vacuum at room temperature for 18 h. The resulting powder was then heated in a tube furnace in a flowing N$_2$/H$_2$ (90/10) atmosphere to 660 °C for 2 h.

The ∼20 % Pt/Vulcan carbon standard was from Etek, and the 47.3 % Pt/carbon standard was from TKK. The chemical composition of the catalysts was determined by inductively coupled plasma (ICP) emission spectroscopy performed by Columbia Analytical Services, Inc., and checked by CALI Laboratories, Inc. of Parsippany, NJ, as well as by our own analyses. The Pt/[TaOPO$_4$/VC] catalyst reported here had a composition of 17.8 (±0.5) % Pt, 3.0 (±0.5) % Ta, ∼1 % P, and 71.3 % carbon. Platinum particle sizes were estimated by X-ray diffraction (XRD, Bruker D8 Advance diffractometer [Cu Kα radiation: 40 KV, 40 mA; 1.2° 2 θ min^{-1} step size]) using the Scherrer equation, with the following results: 2.4 nm for the Pt/[TaOPO$_4$/VC] catalyst, 3.5 nm for the 20 % Pt/Vulcan carbon catalyst, and 2.8 nm for the 47.3 % Pt/carbon catalyst. The physical morphology of Pt/[TaOPO$_4$/VC] catalysts was surveyed with high-area HAADF-STEM using a JEOL 2100F STEM.

Our experimental and computational methods for the RDE methodology have been reported elsewhere in detail, including preparation of the catalyst inks and the catalyst thin films, electrochemical details for cyclic voltammetry measurements and RDE measurements, as well as the formulas used for determination of the catalyst Pt electrochemical surface area (ECSA) and the ORR activity in terms of mass-specific and area-specific activity.[9,19] The best ink formulation for the Pt/[TaOPO$_4$/VC] catalysts was found to be one with only water as the solvent.

SUPPORTING INFORMATION AVAILABLE
RDE thin-film limit justification for the Pt/[TaOPO$_4$/VC] electrocatalyst, derived equations for the calculation of Pt ECSA, kinetic current, and mass-specific and area-specific activities. This material is available free of charge via the Internet at http://pubs.acs.org.

AUTHOR INFORMATION

Corresponding Author:
*To whom correspondence should be addressed. Phone: 202-404-1825. Fax: 202-404-8119. E-mail: yannick.garsany@nrl.navy.mil.

REFERENCES

(1)   Gasteiger, H. A.; Kocha, S. S.; Sompalli, B.; Wagner, F. T. Activity Benchmarks and Requirements for Pt, Pt-Alloy, and

Non-Pt Oxygen Reduction Catalysts for PEMFCs. *Appl. Catal., B* **2005**, *56*, 9–35.

(2) Mathias, M. F.; et al. Two Fuel Cell Cars in Every Garage? *Electrochem. Soc. Interface* **2005**, *14*, 24–35.

(3) Tang, H.; Qi, Z. G.; Ramani, M.; Elter, J. F. PEM Fuel Cell Cathode Carbon Corrosion Due to the Formation of Air/Fuel Boundary at the Anode. *J. Power Sources* **2006**, *158*, 1306–1312.

(4) Ioroi, T.; Siroma, Z.; Fujiwara, N.; Yamazaki, S.; Yasuda, K. Sub-Stoichiometric Titanium Oxide-Supported Platinum Electrocatalyst for Polymer Electrolyte Fuel Cells. *Electrochem. Commun.* **2005**, *7*, 183–188.

(5) Lim, D. H.; Lee, W. D.; Choi, D. H.; Kwon, H. H.; Lee, H. I. The Effect of Cerium Oxide Nanoparticles on a Pt/C Electrocatalyst Synthesized by a Continuous Two-Step Process for Low-Temperature Fuel Cell. *Electrochem. Commun.* **2008**, *10*, 592–596.

(6) Elezovic, N. R.; Babic, B. M.; Radmilovic, V. R.; Gojkovic, S. L.; Krstajic, N. V.; Vracar, L. M. Pt/C Doped by MoOx as the Electrocatalyst for Oxygen Reduction and Methanol Oxidation. *J. Power Sources* **2008**, *175*, 250–255.

(7) Elezovic, N. R.; Babic, B. M.; Radmilovic, V. R.; Vracar, L. M.; Krstajic, N. V. Synthesis and Characterization of MoOx–Pt/C and TiOx–Pt/C Nano-Catalysts for Oxygen Reduction. *Electrochim. Acta* **2009**, *54*, 2404–2409.

(8) Sasaki, K.; Zhang, L.; Adzic, R. R. Niobium Oxide-Supported Platinum Ultra-Low Amount Electrocatalysts for Oxygen Reduction. *Phys. Chem. Chem. Phys.* **2008**, *10*, 159–167.

(9) Baturina, O. A.; Garsany, Y.; Zega, T. J.; Stroud, R. M.; Schull, T.; Swider-Lyons, K. E. Oxygen Reduction Reaction on Platinum/Tantalum Oxide Electrocatalysts for Pem Fuel Cells. *J. Electrochem. Soc.* **2008**, *155*, B1314–B1321.

(10) Lee, K. H.; Kwon, K.; Roev, V.; Yoo, D. Y.; Chang, H.; Seung, D. Synthesis and Characterization of Nanostructured PtCo–CeOx/C for Oxygen Reduction Reaction. *J. Power Sources* **2008**, *185*, 871–875.

(11) Chhina, H.; Campbell, S.; Kesler, O. Ex Situ and in Situ Stability of Platinum Supported on Niobium-Doped Titania for PEMFCs. *J. Electrochem. Soc.* **2009**, *156*, B1232–B1237.

(12) Xiong, L.; More, K. L.; He, T. Syntheses, Characterization, and Catalytic Oxygen Electroreduction Activities of Carbon-Supported PTW Nanoparticle Catalysts. *J. Power Sources* **2010**, *195*, 2570–2578.

(13) Huang, S.-Y.; Ganesan, P.; Popov, B. N. Electrocatalytic Activity and Stability of Niobium-Doped Titanium Oxide Supported Platinum Catalyst for Polymer Electrolyte Membrane Fuel Cells. *Appl. Catal., B* **2010**, *96*, 224–231.

(14) Horsley, J. A. Molecular-Orbital Study of Strong Metal-Support Interaction between Platinum and Titanium-Dioxide. *J. Am. Chem. Soc.* **1979**, *101*, 2870–2874.

(15) Bouwman, P. J.; Dmowski, W.; Stanley, J.; Cotten, G. B.; Swider-Lyons, K. E. Platinum-Iron Phosphate Electrocatalysts for Oxygen Reduction in PEMFCS. *J. Electrochem. Soc.* **2004**, *151*, A1989–A1998.

(16) Lyons, K. S.; Baturina, O. A.; Garsany, Y. Oxygen Reduction on Oxide- and Phosphate-Supported Noble Metal Catalysts. In *Catalysts for Oxygen Electroreduction-Recent Developments and New Directions*; He, T., Ed.; Transworld Research Network: Trivandrum, India, 2009; 169–193.

(17) Kreuer, K. D. Proton Conductivity: Materials and Applications. *Chem. Mater.* **1996**, *8*, 610–641.

(18) Paulus, U. A.; Schmidt, T. J.; Gasteiger, H. A.; Behm, R. J. Oxygen Reduction on a High-Surface Area Pt/Vulcan Carbon Catalyst: A Thin-Film Rotating Ring-Disk Electrode Study. *J. Electroanal. Chem.* **2001**, *495*, 134–145.

(19) Garsany, Y.; Baturina, O. A.; Kocha, S. S.; Swider-Lyons, K. E. Experimental Methods for Quantifying the Activity of Platinum Electrocatalysts for the Oxygen Reduction Reaction. *Anal. Chem.* **2010**, in press, DOI: 10.1021/ac100306c.

(20) Paulus, U. A.; Wokaun, A.; Scherer, G. G.; Schmidt, T. J.; Stamenkovic, V.; Radmilovic, V.; Markovic, N. M.; Ross, P. N. Oxygen Reduction on Carbon-Supported Pt–Ni and Pt–Co Alloy Catalysts. *J. Phys. Chem. B* **2002**, *106*, 4181–4191.

(21) Stamenkovic, V.; Schmidt, T. J.; Ross, P. N.; Markovic, N. M. Surface Composition Effects in Electrocatalysis: Kinetics of Oxygen Reduction on Well-Defined Pt$_3$Ni and Pt$_3$Co Alloy Surfaces. *J. Phys. Chem. B* **2002**, *106*, 11970–11979.

(22) Baturina, O. A.; Gould, B. D.; Garsany, Y.; Swider-Lyons, K. E. Insights of SO$_2$ Poisoning of Pt$_3$Co/VC and Pt/VC Fuel Cell Catalysts. *Electrochim. Acta* **2010**, In press.

(23) Swider-Lyons, K. E.; Teliska, M. E.; Baker, W. S.; Bouwman, P. J.; Pietron, J. J. Leveraging Metal–Support Interactions to Improve the Activity of PEMFC Cathode Catalysts. *ECS Trans.* **2006**, *1*, 97–105.

(24) Waje, M. M.; Li, W.; Chen, Z.; Larsen, P.; Yan, Y. Effect of Scan Range on Pt Surface Area Loss in Potential Cycling Experiments. *ECS Trans.* **2007**, *11*, 1227–1233.

(25) Baker, W. S.; Pietron, J. J.; Teliska, M. E.; Bouwman, P. J.; Ramaker, D. E.; Swider-Lyons, K. E. Enhanced Oxygen Reduction Activity in Acid by Tin-Oxide Supported Au Nanoparticle Catalysts. *J. Electrochem. Soc.* **2006**, *153*, A1702–A1707.

(26) Gatewood, D.; Ramaker, D. E.; Sasaki, K.; Swider-Lyons, K. E. Establishing the Mechanism for Oxygen Reduction on Au/SnOx Using in Situ X-Ray Absorption Spectroscopy. *ECS Trans.* **2007**, *11*, 271–276.

(27) Wang, Y.; Ren, J. W.; Deng, K.; Gui, L. L.; Tang, Y. Q. Preparation of Tractable Platinum, Rhodium, and Ruthenium Nanoclusters with Small Particle Size in Organic Media. *Chem. Mater.* **2000**, *12*, 1622–1627.